Nonlocal conductivity in the vortex-liquid regime of a two-dimensional superconductor

Rachel Wortis
Department of Physics, University of Illinois at Urbana-Champaign, 1110 West Green Street, Urbana, Illinois 61801 and Bell Laboratories, Murray Hill, New Jersey 07974

David A. Huse*
Bell Laboratories, Murray Hill, New Jersey 07974
(Received 29 April 1996)

We have simulated the time-dependent Ginzburg-Landau equation with thermal fluctuations, to study the nonlocal dc conductivity of a superconducting film. Having examined points in the phase diagram at a wide range of temperatures and fields below the mean field upper critical field, we find a portion of the vortex-liquid regime in which the nonlocal Ohmic conductivity in real space is negative over a distance several times the spacing between vortices. The effect is suppressed when driven beyond linear response. Earlier work had predicted the existence of such a regime, due to the high viscosity of a strongly correlated vortex liquid. This behavior is clearly distinguishable from the monotonic spatial falloff of the conductivity in the higher-temperature or field regimes approaching the normal state. The possibilities for experimental study of the nonlocal transport properties are discussed. [S0163-1829(96)05338-6]

I. INTRODUCTION

In this paper we present the results of a computer simulation designed to study the nonlocal dc conductivity of a two-dimensional (thin-film) type-II superconductor. The meaning of nonlocal in this context can be seen in the standard expression connecting the local current density in a material, **J**, to the local electric field, **E**, in the linear (Ohmic) regime:

$$J_\mu(\mathbf{r}) = \int \sigma_{\mu\nu}(\mathbf{r},\mathbf{r}')E_\nu(\mathbf{r}')d\mathbf{r}'. \tag{1.1}$$

When the conductivity $\sigma(\mathbf{r},\mathbf{r}')$ is nonzero for $\mathbf{r}\neq\mathbf{r}'$, then it is nonlocal. In a translationally invariant system, the nonlocal conductivity can only be a function of the difference $(\mathbf{r}-\mathbf{r}')$. The Fourier transform of the conductivity equation is then $J_\mu(\mathbf{k})=\sigma_{\mu\nu}(\mathbf{k})E_\nu(\mathbf{k})$. The nonlocal conductivity we are discussing here is a different phenomenon from Pippard's nonlocal relation between the supercurrent and the vector potential below T_c in a type-I superconductor.[1] In particular, we are interested in the nonlocal conductivity in the resistive vortex-liquid regime of a type-II superconductor in a magnetic field.

All materials exhibit nonlocal transport properties on some length scale. Normal metals behave nonlocally on length scales less than or of the order of the inelastic mean free path. In superconductors, however, the scale of the nonlocality can be much larger. Israeloff *et al.*[2] have measured effects arising from the nonlocal resistivity due to superconducting fluctuations just above T_c in one-dimensional rings of type-I material. The observed behavior, predicted by Glazman *et al.*,[3] arises from the correlations of the superconducting order parameter.

In the mixed state of a type-II superconductor, the presence of vortices provides another mechanism for nonlocal resistivity. When a current $\mathbf{J}(\mathbf{r}')$ exerts Lorentz and Magnus forces on a vortex segment at $\mathbf{r}'$ and causes it to move, this vortex motion can in turn cause vortex segments at $\mathbf{r}$ to move, through vortex interactions, connections, or entanglement. The motion of the vortices at $\mathbf{r}$ produces phase slip and electric fields at $\mathbf{r}$, as described by the Josephson relation, completing a nonlocal relation between current and electric field. In the vortex-liquid regime, this tendency of a moving vortex to drag along nearby vortices can be understood in terms of a vortex-liquid viscosity, as discussed by Marchetti and Nelson.[4] Using nonuniform applied currents, Safar *et al.*[5] have observed nonlocal resistivity over length scales of tens of micrometer in bulk crystals of the high-temperature superconductor $YBa_2Cu_3O_7$ (YBCO). These results were discussed phenomenologically by Huse and Majumdar.[6]

In a recent paper with Mou and Dorsey,[7] we examined the nonlocal dc transport properties throughout the phase diagram of a type-II superconductor, using analytic calculations where possible and proposing phenomenological arguments elsewhere. In particular, we predicted that the wave-vector-dependent dc electrical conductivity, $\sigma(k)$, of a type-II superconductor would have a nonmonotonic dependence on k in a certain region of the phase diagram: For those values of magnetic field and temperature at which there exists a well-correlated liquid of field induced vortices, the dc conductivity as a function of increasing wave vector k was argued to increase for small values of k and then decrease at large values of k. The increase in the conductivity at small k arises from viscous drag between vortices[4] which impedes their relative motion and therefore decreases their contribution to resistance in a nonuniform current. However, when the length scale of the nonuniformity in the current is smaller than the intervortex spacing (high k), the conductivity is more determined by the short-distance correlations of the superconducting order parameter, rather than the vortex interactions. In this short-distance regime the behavior is as in zero magnetic field: The conductivity decreases with increasing k.

Because this effect is only expected to appear in a regime with strong correlations and fluctuations, analytical calculations do not appear feasible. In the present paper we report on computer simulations of the time-dependent Ginzburg-Landau (TDGL) equation in two dimensions which allow us to study the nonlocal dc conductivity both in real space and in wave vector space as a function of magnetic field H and temperature T. We have indeed observed the nonmonotonic k dependence in the vortex-liquid regime, as expected.[7]

One way to probe the nonlocal transport properties experimentally is to apply currents that are nonuniform on the appropriate length scale.[8] This has been done in two types of experiments, so far. Israeloff *et al.*[2] have made 3-μm-size wire loops, applied the current asymmetrically, and measured resistances as a function of a magnetic flux passing through the loop. Safar *et al.*[5] have applied contacts to both sides of 10–50-μm-thick YBCO samples, measuring effects due to the nonuniformity of the current across the sample. This latter experiment detected the nonlocal resistivity along the direction parallel to the vortex lines, due to the lines having integrity (not breaking) across the sample in a portion of the vortex-liquid regime. The present work indicates that the phenomenon is quite general, and could be studied in superconductors of any dimensionality. What is required is to be able to apply nonuniform currents and measure voltages on length scales of order the appropriate correlation length of the superconductor. With modern microfabrication techniques (and/or possibly using scanning-tip probes) this should be feasible for a broader range of materials and geometries than those used in the two experiments discussed above. What would be best would be an experiment that simultaneously and quantitatively probes a range of length scales, so that the dependence of the transport properties on length scale (and other parameters) can be systematically studied.[9] We hope the results reported below help motivate such studies.

An outline of this paper is as follows. Section II describes the simulation. Section III outlines the phase diagram of a two-dimensional superconductor, providing a context for our results. Section IV describes the conductivity we observe in both real and wave vector space in the different regimes of the phase diagram. Finally, in Sec. V, the results are discussed, both in the context of earlier work and in terms of possible experiments.

II. SIMULATION

We wish to study the nonlocal conductivity of a two-dimensional (thin-film) sample of a strongly type-II superconductor. We begin with the time-dependent Ginzburg-Landau (TDGL) equation (SI units):

$$\Gamma^{-1}\left(\partial_t + i\frac{e^*}{\hbar}\Phi\right)\Psi = \frac{\hbar^2}{2m^*}\left(\nabla - i\frac{e^*}{\hbar}\mathbf{A}\right)^2\Psi - a\Psi - b|\Psi|^2\Psi + \zeta(\mathbf{r},t). \tag{2.1}$$

$\Psi(\mathbf{r},t)=\psi(\mathbf{r},t)e^{i\phi(\mathbf{r},t)}$ is the superconducting order parameter. Γ is the kinetic coefficient for the relaxation of the order parameter towards equilibrium; it is assumed to be real. m^* is the effective mass of a Cooper pair and $e^*=2e$ is the charge of a Cooper pair. The noise ζ is Gaussian distributed and δ-function correlated, with the coefficient given by the fluctuation-dissipation theorem,

$$\langle \zeta^*(\mathbf{r},t)\zeta(\mathbf{r}',t')\rangle = 2\Gamma^{-1}k_BT\delta^{(d)}(\mathbf{r}-\mathbf{r}')\delta(t-t'). \tag{2.2}$$

Φ and $\mathbf{A}$ are the scalar and vector potentials, respectively. We consider the strongly type-II (large κ) limit, where the order-parameter fluctuations are much stronger than the magnetic field fluctuations. Thus we use a uniform, static magnetic field.

To simplify this equation we rescale: Energy is measured in units of $|a|$. We work only below the mean field T_c, and so we set $a=-1$. The order parameter magnitude is measured in units of $\sqrt{|a|/b}$, its equilibrium value at zero noise and zero magnetic field; therefore, $b=+1$. Length is measured in units of $\xi=\hbar/\sqrt{2m^*|a|}$, the order-parameter correlation length at zero noise and zero magnetic field, so $\hbar^2/2m^*=1$. Magnetic flux is measured in units such that the flux quantum is 2π; that is, $e^*/\hbar=1$. Time is measured in units of $1/\Gamma|a|$, so $\Gamma=1$. We also take $k_B=1$. The parameters remaining are the temperature, now measured in units of $|a|$, and the magnetic field in units of flux quanta per area $2\pi\xi^2$ or, equivalently, in units of the mean-field upper critical field, $H_{c2}^{\mathrm{MF}}(T)$. The theory also needs an ultraviolet cutoff, which we realize in the simulations by discretizing space. Note that when our rescaled temperature is large ($T\gg 1$), this means $k_BT\gg -a>0$, which is the regime of strong thermal fluctuations *below* the mean field transition temperature, T_c^{MF}.

The rescaled equation is

$$(\partial_t + i\Phi)\Psi = (\nabla - i\mathbf{A})^2\Psi + \Psi - |\Psi|^2\Psi + \zeta. \tag{2.3}$$

To solve this equation, we discretize space and time. The film is approximated by a square lattice with spacing one in the rescaled units. Time is divided into a series of time steps. The length of these time steps must be decreased at higher-temperatures in order to obtain accurate steady-state results and avoid numerical instabilities. We used time steps in the range of 0.2 to 0.02 rescaled time units for temperatures ranging from 0 to 1, respectively.

Taking advantage of the gauge invariance of the equation, we work in terms of only gauge-invariant quantities, namely, the order-parameter magnitudes at each site of the lattice, $\psi(\mathbf{r})$, and the gauge-invariant phase differences along each nearest-neighbor link, θ, defined by

$$\theta(\mathbf{r},\mathbf{r}') = \phi(\mathbf{r}') - \phi(\mathbf{r}) - \int_{\mathbf{r}}^{\mathbf{r}'}\mathbf{A}\cdot d\boldsymbol{l}, \tag{2.4}$$

where $\mathbf{r}$ and $\mathbf{r}'$ are adjacent lattice points and the integral is along the straight line between them. Derivatives are approximated using differences, and only differences up to one time step and two lattice spacings are kept; this is the minimum needed to approximate the derivatives appearing in the TDGL equation.

We use periodic boundary conditions in both the x and y directions, giving effectively a toroidal surface. We begin with random initial conditions, setting the gauge-invariant phase difference to a random number between $-\pi$ and π on three of the four links surrounding each plaquette; the phase difference on the last link is then determined uniquely

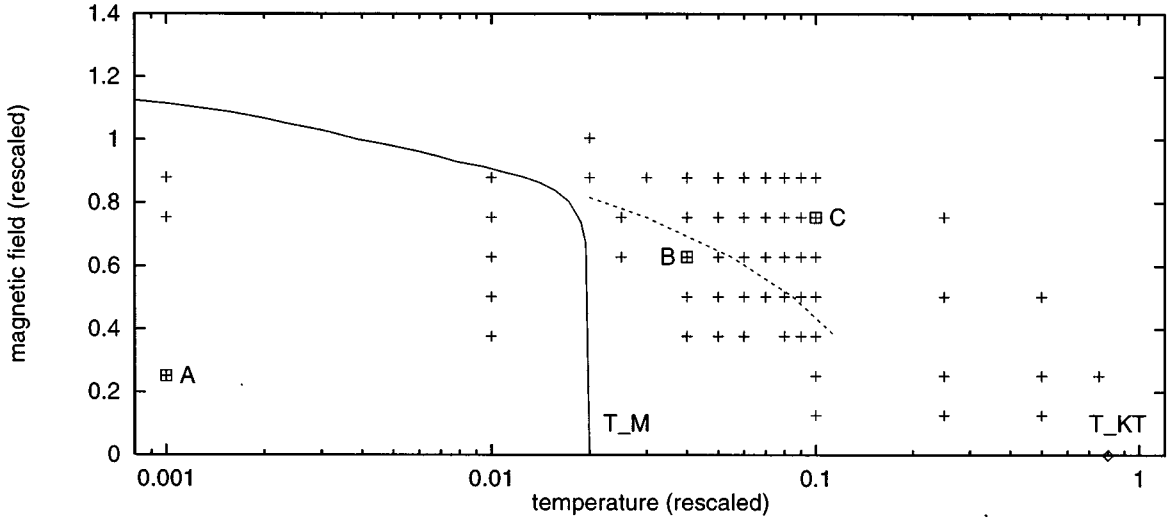

FIG. 1. Sketch of the phase diagram of the model thin-film superconductor we have simulated. Note the logarithmic scale on the temperature axis. The solid curve is a rough estimate of the melting boundary based on our estimate of T_{KT} (marked with a diamond) and Ref. 12. The points we have studied are marked with crosses, and representative points *A*, *B*, and *C* are marked with squares. Negative nonlocal conductivity was observed for the points below the dashed line. The near intersection of the dashed line and the (solid) melting curve may not be significant, because both have large uncertainties in their precise locations (see text).

(modulo 2π) by the magnetic flux passing through the plaquette. The order parameter magnitude begins at the small, spatially uniform value of 0.01.

Our goal is to study the conductivity. To do this we apply an electric field and measure the electrical current. The TDGL equation in this type-II limit only involves the supercurrent due to the paired electrons that produces enhanced conductivity over that of the normal state. The supercurrent, in our rescaled units, is

$$\mathbf{J}_s = 2\,\mathrm{Im}\,\{\Psi^*(\nabla - i\mathbf{A})\Psi\}. \tag{2.5}$$

This we also discretize as described above, so the supercurrent is defined on each nearest-neighbor link of the lattice as

$$\mathbf{J}_s(\mathbf{r},\mathbf{r}') = 2\,\psi(\mathbf{r})\,\psi(\mathbf{r}')\sin[\,\theta(\mathbf{r},\mathbf{r}')\,]. \tag{2.6}$$

In addition to this supercurrent, there is also a normal current which we will assume is simply local and Ohmic: $\mathbf{J}_n(\mathbf{r}) = \sigma_n \mathbf{E}(\mathbf{r})$, where σ_n is the normal-state conductivity.

We generally apply an electric field that is uniform in the y direction, parallel to $\hat{\mathbf{x}}$ and given by a δ function along x:

$$\mathbf{E} = E_0\,\delta(x)\hat{\mathbf{x}}. \tag{2.7}$$

On the lattice this δ function is realized by applying the electric field only between two adjacent columns of lattice sites. In this geometry the resulting current is also parallel to $\hat{\mathbf{x}}$ and, in the linear response regime, is given by

$$J(x) = E_0 \int dy\,\sigma_{xx}(x,y) = E_0\,\sigma_{xx}(x,k_y=0). \tag{2.8}$$

Thus we measure the dependence of the nonlocal conductivity on the spacing x for conditions that are uniform along y ($k_y = 0$). By Fourier transforming on x we also obtain $\sigma_{xx}(k_x, k_y = 0)$.

III. PHASE DIAGRAM

Our simulation is designed to represent a superconducting film with thickness less than the bulk order-parameter correlation length. When there is no applied magnetic field, such a system is expected to undergo a Kosterlitz-Thouless transition at a temperature T_{KT}.[10] Below this temperature there are bound pairs of vortices, but no free vortices and therefore no Ohmic resistance to a uniform dc current. Above T_{KT}, there are free vortices, whose mobility results in a nonzero resistivity.

When a magnetic field is applied perpendicular to the plane of such a film, the flux is not expelled. At low-temperatures, a triangular vortex lattice forms. Above the melting temperature $T_M(H)$, this lattice becomes unstable to dislocations and melts. At intermediate magnetic fields, i.e., much less than the mean field $H_{c2}^{\mathrm{MF}}(T)$ but greater than one flux quantum per magnetic penetration length squared, T_M is expected to be only weakly field dependent.[11] In the limit of a normal-state sheet resistance much larger than the quantum of resistance, $\hbar/(e^*)^2$, $T_M = (0.026 \pm 0.008)T_{\mathrm{KT}}$ in this intermediate-field regime.[11] When the temperature is rescaled as we have done, this relation between T_M and T_{KT} holds for films with a smaller sheet resistance as well. At higher magnetic fields, near the mean field $H_{c2}^{\mathrm{MF}}(T)$, $T_M \propto [H_{c2}(0) - H]^2$ for Ginzburg-Landau theory with thermal fluctuations.[11] The locations of the phase transitions are roughly sketched in Fig. 1.

To estimate the zero-field transition temperature, we used a finite-size scaling analysis of the order-parameter phase correlations, obtaining $T_{\mathrm{KT}} = 0.8 \pm 0.1$, which implies $T_M = 0.02 \pm 0.01$ in the intermediate-field regime. We did not attempt to directly estimate T_M by looking for the melting transition in our simulations. We also raised the applied field until the zero-temperature equilibrium order-parameter mag-

nitude dropped to zero to find that $H_{c2}(T=0)=1.18\pm0.02$. In the continuum, $H_{c2}(T=0)=1$ in our rescaled units; the increase to roughly 1.2 is due to our approximating the continuum by a lattice with spacing ξ and approximating the spatial derivative with the lowest-order difference. We expect other quantities are also quantitatively shifted small amounts by these approximations. In particular, the precise values we obtain for the conductivity are likely to be affected. However, as we are focusing on trends related to the variation of x, k, H, and T rather than on precise numerical values, these shifts are not expected to affect our conclusions.

IV. RESULTS

We studied points in the phase diagram in the field range $0\leqslant H\leqslant 1.2$ and the temperature range $0\leqslant T\leqslant 1$ as shown in Fig. 1. At most points we studied, all the vortices present were field induced. Thermally induced vortex-antivortex pairs were observed only for $T\geqslant 0.1$. However, the number of field-induced vortices was much greater than that of thermally induced vortices for temperatures up to 0.5 at the nonzero field values studied.

We saw three characteristic behaviors for the nonlocal conductivity. The points A, B, and C shown in Fig. 1 are chosen as clear examples of these behaviors. Point A, at $T=0.001$ and $H=2\pi/25$, is representative of what is seen in the ordered phases at very low temperatures and fields, including $T=0$ and $H=0$. Point B, at $T=0.04$ and $H=\pi/5$, is representative of the well-correlated vortex-liquid regime, intermediate in both temperature and field. Finally, point C, at $T=0.1$ and $H=6\pi/25$, is representative of high-temperature and high-field behavior.

In a linear response, the nonlocal conductivity in real space, $\sigma_{xx}(x,k_y=0)$, for the characteristic points is as follows (Fig. 2): At point C, we see a conductivity which is sharply peaked around $x=0$, falling off exponentially to zero with a length scale of order the correlation length. This behavior is in qualitative agreement with the high-temperature behavior obtained analytically from lowest-order fluctuations about the mean-field normal state.[7] At point B the conductivity still has a sharp peak at $x=0$ of similar width to that at point C, but it then drops *below* zero over a distance of few intervortex spacings before returning to zero. This is the negative nonlocal conductivity expected in this well-correlated vortex-liquid regime.[7] At both points B and C the conductivities and correlation lengths are all finite, so the numerical results for a finite sample that is large compared to all correlation lengths do not show finite-size effects and thus are a faithful representation of a much larger sample.

In the ordered phases the uniform conductivity is infinite. In the Meissner phase ($H=0$) this is true for the continuum system as well, while for the vortex-lattice phase the infinite uniform ($k=0$) conductivity is due to weak pinning of the vortices to our numerically imposed lattice that impedes the ''flux flow'' that would occur for the continuum system. To avoid this divergence, instead of applying only the δ-function electric field (2.7) as was done at points B and C, at point A we also apply a compensating spatially uniform electric field that cancels the uniform ($k=0$) component coming from the δ function. This means we do not measure

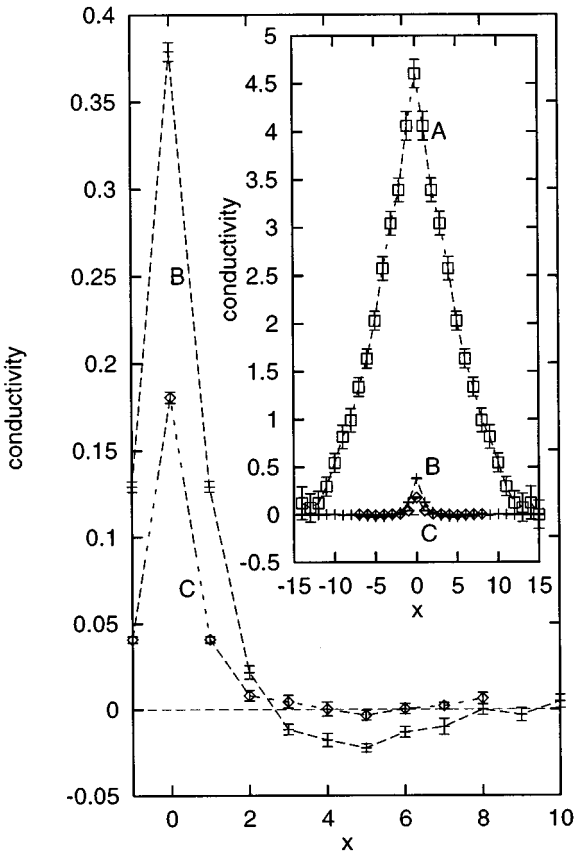

FIG. 2. Conductivity $\sigma_{xx}(x,k_y=0)$ as a function of position x at the points B and C indicated in the phase diagram (Fig. 1). Note the negative nonlocal conductivity for B. Inset also includes point A; the vertical zero is shifted for the data from point A only (see text). The local normal-state contribution to the conductivity at $x=0$ has not been included here.

the very large $k=0$ part of the conductivity and the data for point A in the inset to Fig. 2 consequently has an arbitrary x-independent vertical shift. The conductivity vs x shows a broad peak at the origin, with a width and magnitude proportional to the linear sample size and a shape well fit by a parabola centered on the column opposite to where the δ-function component of the electric field is applied.

Still in linear response, but now in k space (see Fig. 3), at point C, the conductivity $\sigma_{xx}(k_x,k_y=0)$ falls monotonically from its value at $k_x=0$. At point B the conductivity rises from its value at $k=0$ to a maximum at a wave vector roughly corresponding to the inverse of the vortex spacing and then declines. At point A (inset) the conductivity falls off monotonically like $1/k^2$, as expected.[7]

At point B, when the system is driven beyond linear response, the effect is to reduce the magnitude both of the peak in $\sigma(x)$ and of the negative regions. In k space, the effect is to suppress the nonmonotonicity. Figure 4 shows $\sigma(k)$ for a series of applied electric fields of increasing magnitude. Here in the nonlinear regime we apply the δ-function electric field (2.7), measure $J_s(x)$, define the nonlocal and nonlinear conductivity as $\sigma(x)=J_s(x)/E_0$, and show its Fourier transform in Fig. 4. The higher electric fields produce a strong shear flow in the vortex liquid, which apparently reduces the effective viscosity of the vortex liquid.

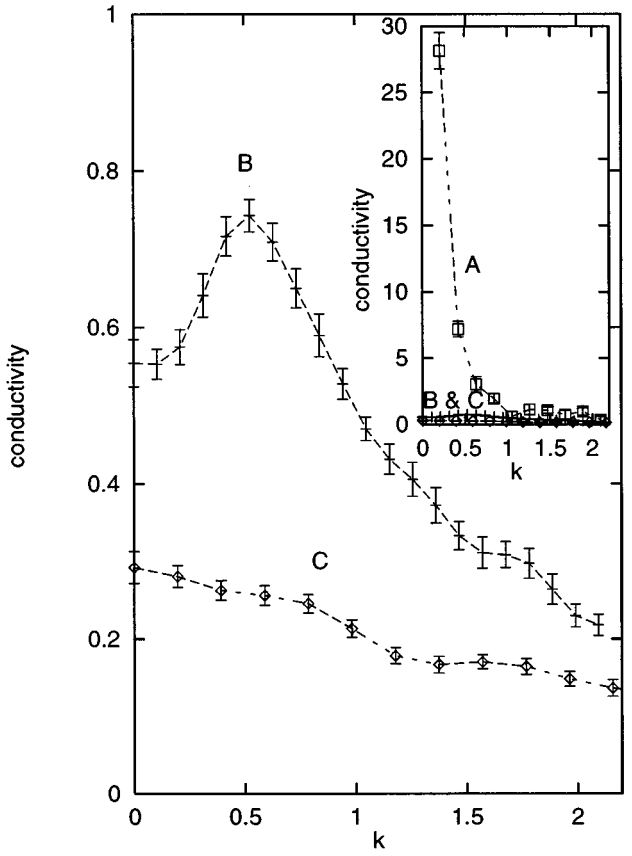

FIG. 3. Conductivity as a function of wave vector at the points *B* and *C*. Inset includes point *A*. These data are simply the Fourier transforms of those in Fig. 2, so the *k*-independent normal-state contribution is not included.

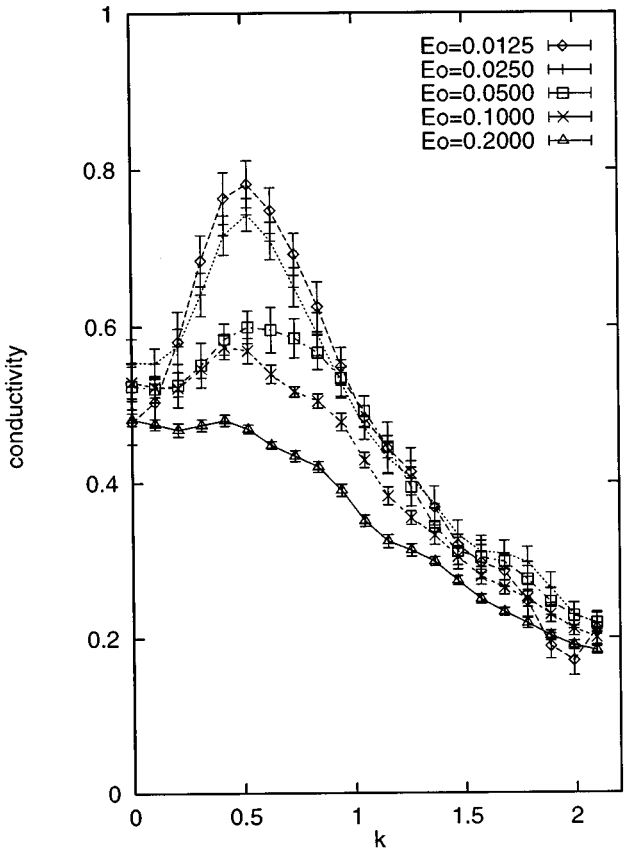

FIG. 4. Nonlinear conductivity (see the text for a precise definition) as a function of wave vector in the vortex liquid at the point *B* for five values of electric field: 0.0125, 0.025, 0.05, 0.1, and 0.2.

For points in the vortex liquid below the dashed line in Fig. 1, the nonlocal conductivity in k space showed nonmonotonicity significantly outside the statistical errors. Above this line nonmonotonic behavior is still observed at many points; however, it is not possible to distinguish between true nonmonotonicity and statistical noise at these points, given the level of accuracy of the present data. Thus the dashed line is actually a lower bound on the true boundary between monotonic and nonmonotonic $\sigma(k)$. This boundary is only a crossover, not a phase transition; it is roughly where the correlation length of the conductivity (the range of the nonlocal conductivity in real space) becomes comparable to the intervortex spacing. An interesting question is whether this boundary, like the melting line, intersects the zero-field axis at a temperature below T_{KT}. Following this line to lower fields in our simulations is difficult. It goes to higher temperatures where smaller time steps are required for numerical stability. Also, to study lower fields, larger samples are required in order to include a sufficient number of field induced vortices and to probe distances well beyond the intervortex spacing. Following the line to lower temperatures is also difficult. As it approaches the melting line, nonlinear response sets in at progressively lower applied electric fields, and longer runs are required in order to obtain good signal-to-noise ratios in the linear response regime.

V. DISCUSSION

To discuss the phenomena we have observed, and in particular to connect with experimental possibilities, it is useful to speak in terms of resistivity. $\rho(\mathbf{k})$ is simply $\sigma(\mathbf{k})^{-1}$, and $\rho(\mathbf{r})$ is its Fourier transform:

$$E_{\mu}(\mathbf{r}) = \int \rho_{\mu\nu}(\mathbf{r}-\mathbf{r}')J_{\nu}(\mathbf{r}')d\mathbf{r}'. \tag{5.1}$$

When $\sigma_n \ll \sigma_s$, $\rho(k) = 1/[\sigma_n + \sigma_s(k)] \sim \rho_s(k) - \sigma_n[\rho_s(k)]^2$, and when $\sigma_n \gg \sigma_s$, $\rho(k) \sim \rho_n - \sigma_s(k)\rho_n^2$, where $\rho_s(k) = 1/\sigma_s(k)$ and $\rho_n = 1/\sigma_n$.

The resistivity in real space, $\rho_{xx}(x, k_y = 0)$, for the case of very low normal-state conductivity is sketched in Fig. 5 using the nonmonotonic $\sigma_s(k)$ at point *B* from Fig. 3. This shows the response of a film in the xy plane in a magnetic field parallel to z to a current applied between two closely spaced line contacts parallel to each other and to the y axis, in the geometry shown in Fig. 6. If the current contacts are sufficiently closely spaced to approximate well a δ function in current, the resulting electric field pattern is proportional to $\rho_{xx}(x, k_y = 0)$. The effect is as follows: When a current is applied in the x direction between the two line contacts, the vortices which are positioned between the contacts feel a force in the $-y$ direction. When they move in response to this force, the vortices near to but outside the region in which current is flowing are dragged along. An electric field will be

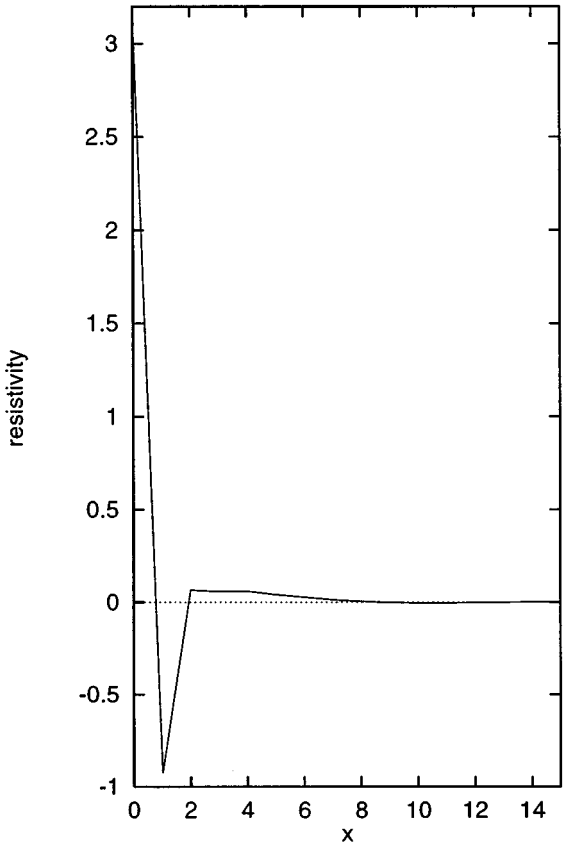

FIG. 5. Nonlocal resistivity $\rho_{xx}(x,k_y=0)$ as a function of position x at the point B in the limit of low normal-state conductivity.

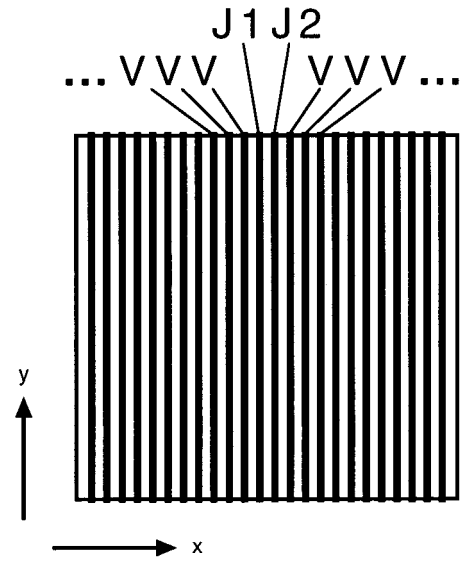

FIG. 6. An idealized proposed experimental geometry. Shown is a superconducting film with parallel line contacts spaced by a distance less than or of order either the intervortex spacing or the correlation length of the superconducting order parameter. The applied current is run from $J1$ to $J2$, and voltage differences between the V contacts are measured.

seen between the two current contacts due to the phase slip caused by the moving vortices as well as simply the flow of normal current. In addition, an electric field of the same sign will be present *outside* the region in which current is flowing, due to phase slip generated by the vortices being dragged by their neighbors. The negative regions in the nonlocal resistivity at short distance are due to the supercurrent being nearly uniform on length scales shorter than the order-parameter correlation length. Thus to get zero net current just outside of the current contacts in Fig. 6 a counterflowing normal current must be present to cancel the supercurrent there. This results in a negative nonlocal resistivity for distance x shorter than the intervortex spacing, as seen in Fig. 5.

Returning to the conductivity measured in our simulation, the negative regions observed in Fig. 2 for point B represent places where the current must flow in the opposite direction to that of the applied electric field in order to keep stationary vortices which would otherwise be dragged along by their moving neighbors. These negative regions in $\sigma(x)$, at x of order the intervortex spacing or more, correspond to the positive regions in $\rho(x)$ for the same x range, and both represent the effect of viscous drag between vortices in the liquid state.

To connect to the work in our earlier paper,[7] in which $\sigma(\mathbf{k})$ was expanded as

$$\sigma_{\mu\nu}(\mathbf{k})=\sigma_{\mu\nu}(0)+S_{\mu\alpha\beta\nu}k_\alpha k_\beta, \tag{5.2}$$

our results indicate that S_{xxxx} is not always negative. At intermediate values of the temperature and field, S_{xxxx} is *positive*, corresponding to a conductivity that increases with increasing wave vector k at small values of k.

Furthermore, we showed previously that, when a hydrodynamic treatment is appropriate, the elements of the S tensor can be written as linear combinations of the elements of the vortex-liquid viscosity tensor defined in the theory of Marchetti and Nelson.[4] Specifically, the element S_{xxxx} is proportional to the viscosity due to the variation in the x direction of vortex motion in the y direction. A positive S_{xxxx} corresponds to a positive vortex-liquid viscosity in a well-correlated liquid of field induced vortices.

However, the negative S_{xxxx} values obtained in the high-T and/or high-H regime should not be thought of as negative vortex-liquid viscosities.[12] S does not represent a vortex-liquid viscosity when the system cannot be described hydrodynamically. At high temperatures and/or fields, the correlation length of the conductivity is shorter than the spacing between vortices, and the value of S comes from interactions not on the scale of vortices but on the shorter scale of the order-parameter correlation length. The conductivity decreases with increasing wave vector as in zero magnetic field. One view of this regime is that the vortex-liquid viscosity becomes so small that the other, shorter-length-scale contributions to the nonlocal conductivity dominate, even at small k.

At intermediate fields and/or temperatures when a hydrodynamic picture is applicable, there are actually two regimes: Here we have presented data at intermediate temperatures and nonzero field where there is a well-correlated liquid of field-induced vortices. In this case the positive vortex-liquid viscosity causes moving vortices to drag along other parallel vortices, thereby producing a positive nonlocal resistivity for x of order the intervortex spacing or larger, as in Fig. 5. At temperatures just above the Kosterlitz-Thouless transition in

zero field, on the other hand, there is a neutral liquid of thermally induced vortices and *antivortices*. In this regime, a moving vortex is more likely to drag a nearby *antivortex*, which is attracted to it, than it is to drag one parallel to itself so the usual positive vortex-liquid viscosity instead produces a negative nonlocal resistivity. We have not used our simulation to study this latter regime.

It appears that experimental observation of these nonlocal transport properties of type-II superconducting films is feasible. What is needed? A high normal-state sheet resistance, R_n, would maximize the extent of the fluctuation regime above the melting line, and it would also minimize the contribution of normal currents to measured quantities. Vortex pinning should be weak enough so that the vortex-liquid regime of interest is not strongly pinned. Many different sample geometries could satisfy the basic requirement that the applied current vary on a length scale of order the correlation length of the conductivity. Point contacts in the middle or at the edge of the film would produce two-dimensional current patterns. Line contacts allow one-dimensional patterns, including approximations to step-function or δ-function configurations. The latter is closest to what we have studied in our simulation. Figure 6 shows an arrangement of a series of line contacts parallel to one another with spacings of order of the intervortex spacing (or, for $H=0$, of order the order-parameter correlation length). Current would be run between nearest-neighbor contacts $J1$ and $J2$, and the voltage differences would be measured between the remaining contacts where there is no net current flowing. Alternatively, a step function applied current pattern could be made by passing current between two more widely separated line contacts in Fig. 6.

The three regimes would appear as follows: (C) In the high-temperature or high-field regime, including the normal state, the voltage difference between all V contacts not between the current contacts will be zero, because the resistivity is local on the length scales studied and no current flows there. However, if the contact spacing is less than or of order the order-parameter correlation length, and well below the intervortex spacing, then the negative nonlocal resistivity should be seen as a negative electric field that falls off as one moves away from the current contacts. This latter regime should be what is seen on approaching T_c from above for zero magnetic field. (A) In the low-temperature, low-field regime, below the melting line, assuming the pinning is negligible, the linear-response electric field measured between each pair of neighboring V contacts will be equal and nonzero due to the uniform motion of the vortex lattice induced by the current. This is also assuming the current contacts are centered on the sample so the net torque on the vortex lattice vanishes. (B) In the well-correlated vortex-liquid regime, the electric field a vortex spacing or more from the current flow will be positive, as the vortices in this region are dragged by their neighbors. This electric field will decrease with a vortex-liquid correlation length as one moves away from where the current is flowing.

To estimate the magnitude of the voltages expected, we need a value for the factor $e^*/\hbar\Gamma|a|$ by which we have rescaled the electric potential. An estimate of $\Gamma|a|$ can be obtained by comparing the theoretical expression for the fluctuation conductivity calculated using the time-dependent Ginzburg-Landau equation,

$$\sigma = k_B T \frac{e^2}{\hbar^2} \frac{1}{2\pi\Gamma|a|} \tag{5.3}$$

(in two dimensions), with experimentally obtained values, as shown in the review by Skocpol and Tinkham.[13] The result is a voltage scale of order 10^{-4} V for materials with bulk transition temperatures of order 1 K. This value is the same as that obtained by dividing the characteristic energy $k_B T_c$ by the electron charge. To obtain linear response at point B we had to decrease the voltage one to two orders of magnitude below this scale, thus to the order of microvolts.

As for the current, the factor by which it has been rescaled is $(|a|^{3/2}/b)e^*/\sqrt{2m^*}$. A rough estimate of its scale can be obtained by dividing the voltage scale by the quantum of resistance and by the order-parameter correlation length. The result is in the range $(10^{-2}$–$1)$ A/cm. Thus the relevant current and voltage scales appear to be well within the reach of present experimental technique (although combining this with the small length scales required may be quite a challenge).

To conclude, our simulation has displayed negative nonlocal conductivity in a vortex-liquid regime, which is distinct from the behavior of the vortex lattice and the higher temperature region. We believe that this signature of the well-correlated vortex liquid is experimentally observable and could provide useful information on vortex dynamics and interactions in type-II superconductors.

ACKNOWLEDGMENTS

R.W. gratefully acknowledges support from AT&T as well as helpful discussions with A.J. Leggett and S. Sondhi. D.H. thanks L.I. Glazman and M.A. Moore for discussions.

*Present address: Physics Department, Princeton University, Princeton, NJ 08544.

[1] E.g., see M. Tinkham, *Introduction to Superconductivity* (McGraw-Hill, New York, 1975).

[2] N.E. Israeloff, F. Yu, A.M. Goldman, and R. Bojko, Phys. Rev. Lett. **71**, 2130 (1993); Physica B **194-196**, 1629 (1994); **203**, 454 (1994).

[3] L.I. Glazman, F.W.J. Hekking, and A. Zyuzin, Phys. Rev. B **46**, 9074 (1992).

[4] M.C. Marchetti and D.R. Nelson, Phys. Rev. B **42**, 9938 (1990); Physica C **174**, 40 (1991).

[5] H. Safar *et al.*, Phys. Rev. Lett. **72**, 1272 (1994); Physica C **235**, 2581 (1994).

[6] D.A. Huse and S.N. Majumdar, Phys. Rev. Lett. **71**, 2473 (1993).

[7] C.-Y. Mou, R. Wortis, A.T. Dorsey, and D.A. Huse, Phys. Rev. B **51**, 6575 (1995).

[8] M.H. Theunissen, E. Van der Drift, and P.H. Kes, Phys. Rev. Lett. **77**, 159 (1996) report a closely related experiment. As suggested by Marchetti and Nelson, they pattern superconducting films with alternating strong- and weak-pinning channels and measure the voltages produced by uniform currents. By do-

ing this for various channel widths, they are able to measure the vortex-liquid viscosity for the amorphous Nb_3Ge films in the weak-pinning channels.

[9] P. Santhanam *et al.*, Phys. Rev. Lett. **66**, 2254 (1991) and Y. K. Kwong *et al.*, Phys. Rev. B **44**, 462 (1991) are two experiments that report length-scale-dependent anomalies near the superconducting transition in aluminum wires. The applied current is nominally uniform in these experiments, and we do not see an explanation of their results based on the ideas considered in this paper.

[10] J.M. Kosterlitz and D.J. Thouless, J. Phys. C **6**, 1181 (1973).

[11] D.S. Fisher, Phys. Rev. B **22**, 1190 (1980).

[12] T. Blum and M.A. Moore, Phys. Rev. B **51**, 15 359 (1995).

[13] W.J. Skocpol and M. Tinkham, Rep. Prog. Phys. **38**, 1049 (1975).